doi:10.14311/ppt.2017.3.273
Plasma Physics and Technology **4**(3):273–276, 2017

A REVIEW OF PROGRESS TOWARDS SIMULATION OF ARC QUENCHING IN LIGHTNING PROTECTION DEVICES BASED ON MULTI CHAMBER SYSTEMS.

A. Chusov[a,*], E.Rodikova[a], M. Murmann[b], H. Nordborg[b], R. Fuchs[b]

[a] *Streamer Electric, St Petersburg, 191024, Russia*

[b] *Institute for Energy Technology, HSR, Rapperswil, 8640, Switzerland*

[*] alexander.chusov@streamer.ru

Abstract. Two distinct modes of follow current suppression were observed in multi-chamber systems (MCS) under lightning overvoltage: Zero Quenching (ZQ) and Impulse Quenching (IQ). Sufficiently lower erosion of electrodes and evaporation of discharge chamber walls makes the IQ more preferable as a mechanism of arc quenching. Since experimental search for best MCS design is both difficult and expensive numerical modeling is considered as a prospective method for geometry optimization. Several steps were made towards development of efficient arc model. This article highlights most important results of arc quenching simulation and current status of arc model development.

Keywords: lightning protection, multi-chamber system, arc discharge, plasma simulations, design optimization.

1. Introduction

Nowadays multi-chamber arresters (MCA) (Fig. 1) are considered as prospective solutions for lightning protection of overhead powerlines [1, 2]. MCA consists of spark gap sequence covered by silicone rubber (Fig. 2). During normal grid operation MCA works as an insulator but when lightning overvoltage is applied it causes cascade of spark gap breakdowns. Each gap when triggered operates as a discharge chamber and conducts lightning current along with current of power frequency.

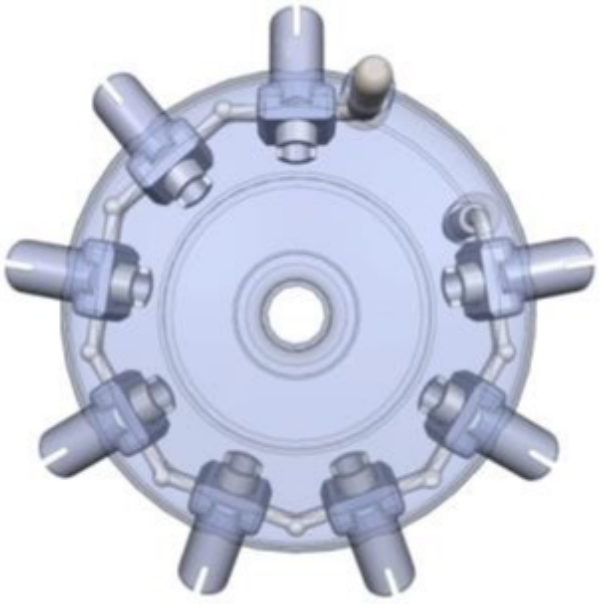

Figure 1. Multi-chamber arrester.

Large current causes strong pressure buildup which in couple with Lorentz force results in outflow of plasma and hot gas leading to arc extinction. Early experiments demonstrated quenching mechanism similar to one employed in circuit breakers - so called Zero Quenching (ZQ): current flows until it passes zero, where cooled arc is quenched (Fig. 3, right). The arcing times are of the order of 10 ms. Large heat loads on electrodes brought by follow current puts an inherent limit on MCA application range. Fortunately another distinct quenching mode - Impulse Quenching (IQ) characterized by sufficiently shorter decay time was discovered in latter experiments. In case of IQ current is suppressed within approximately 0.1 ms (Fig. 3, left), causing significantly less erosion. Further research identified certain MCS geometries capable to perform IQ more efficiently. In order to employ IQ for lightning protection we are looking for optimal design giving best quenching efficiency. Design optimization however was found to be challenging due to difficulty and high expense of tests. To support experimental search numerical simulations of impulse arc quenching in MCA were used to predict better chamber geometry.

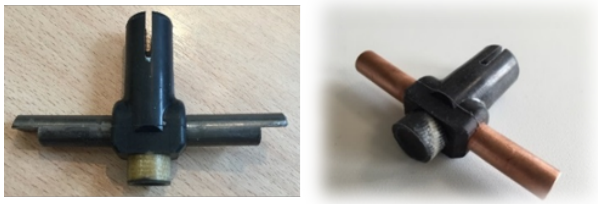

Figure 2. Two examples of MCA discharge chamber design.

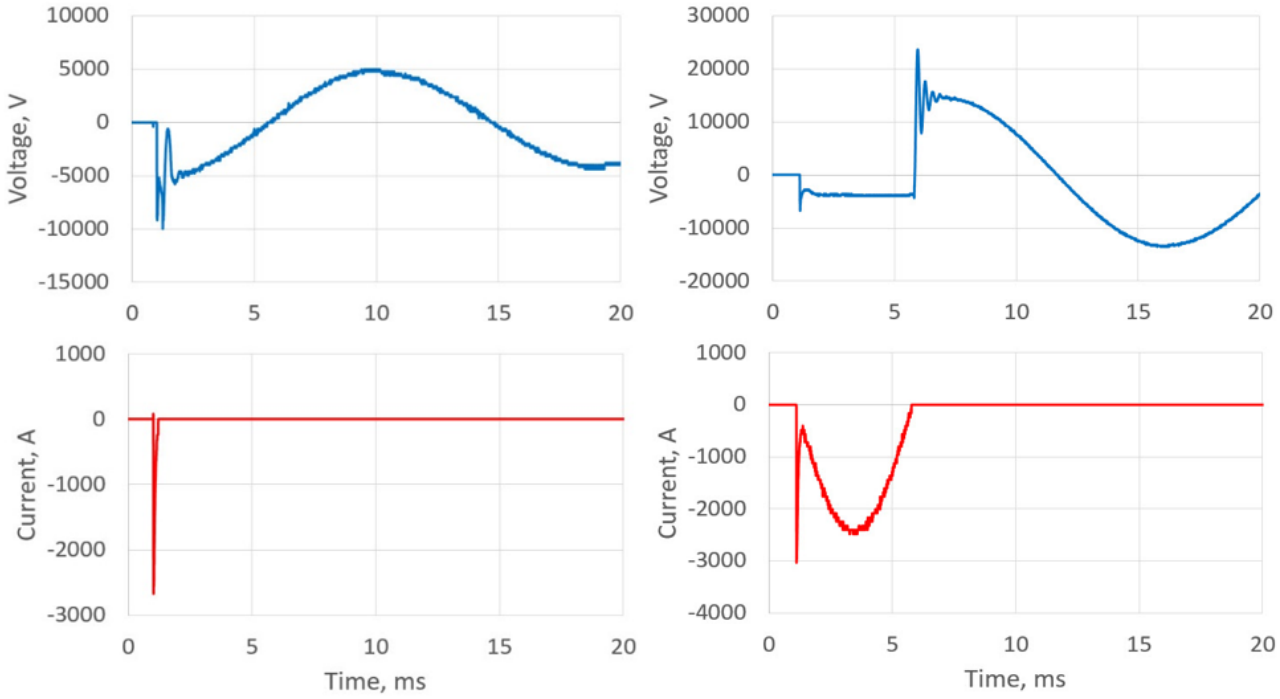

Figure 3. Zero Quenching (ZQ) - right. Impulse Quenching (IQ) - left.

2. Electrical arc simulation

2.1. Basic equations

General approach to arc simulations relies on MHD equations [3]:

$$\frac{\partial \rho}{\partial t} + \nabla \cdot (\rho \mathbf{u}) = 0 \tag{1}$$

$$\frac{\partial(\rho u)}{\partial t} + \nabla(\rho \mathbf{u} \otimes \mathbf{u}) = -\nabla p + \nabla \cdot \tau + [\mathbf{j} \times \mathbf{B}] \tag{2}$$

$$\frac{\partial(\rho h)}{\partial t} + \nabla \cdot (\rho h\ \mathbf{u}) = \frac{\partial p}{\partial t} + \nabla \cdot (\tau \mathbf{u}) + \mathbf{j} \cdot \mathbf{E} + \nabla \cdot (\mathbf{q} + \mathbf{q_{rad}}). \tag{3}$$

Here, ρ represents the mass density, u is the gas velocity, p is the pressure, τ is the viscous part of the stress tensor, and h is the specific enthalpy. The last term of Eq. (3) represents the heat flux, which has been split into a heat conduction q and radiative heat flux q_{rad}. The turbulence is included in the effective viscosity and heat conductivity of the gas. $k - \varepsilon$ turbulence model was used in all simulations ([4]). In order to solve the above set of equations, it is necessary to add state equations,

$$\rho = \rho(p, T) \tag{4}$$

and

$$h = h(p, T). \tag{5}$$

Data for viscosity, thermal and electric conductivity is also needed. The coupling to the electromagnetic field is realized by the Lorentz force $[\mathbf{j} \times \mathbf{B}]$ and the ohmic heating $\mathbf{j} \cdot \mathbf{E}$, where $\mathbf{j}$ is the electric current density,$\mathbf{E}$ is the electric field, and $\mathbf{B}$ is the magnetic induction. The current density is given by

$$\mathbf{j} = \sigma(\mathbf{E} + [\mathbf{u} \times \mathbf{B}]), \tag{6}$$

where σ is the electric conductivity of the plasma. Instead of full Maxwell equations to compute the electric and magnetic fields the magnetostatic approximation was used in this study,

$$\nabla \cdot j = 0 \tag{7}$$

and

$$[\nabla \times \mathbf{B}] = \mu_0 \mathbf{j}. \tag{8}$$

2.2. Material properties

Following the approximation of local thermodynamic equilibrium (LTE), the properties of the plasma only depend on temperature and pressure. It is possible then to precompute all thermodynamic properties and store in the form of lookup tables as described in ([5–7]). For simplicity, electrode erosion and ablation of wall material were neglected, making it possible to consider pure air arc discharge. The pressure dependence was only included for quantities showing strong variation with changing pressure – density $\rho(p, T)$ and the electric conductivity $\sigma(p, T)$ of the plasma.

2.3. Radiation transport

The phenomenon can be modeled by the radiative heat transfer equation for the spectral radiative intensity, which is given by

$$\mathbf{s} \cdot \nabla I_\nu(r, s) = \kappa_\nu [I_\nu^b(T) - I_\nu(r, s)] \tag{9}$$

Here I_ν is the radiative intensity at position r in direction s with frequency ν, κ_ν is the absorption coefficient of the medium, and I_ν^b is the Planck function

$$I_\nu^b(T) = \frac{2h}{c^2} \frac{\nu^3}{e^{\frac{h\nu}{k_B T}} - 1}. \tag{10}$$

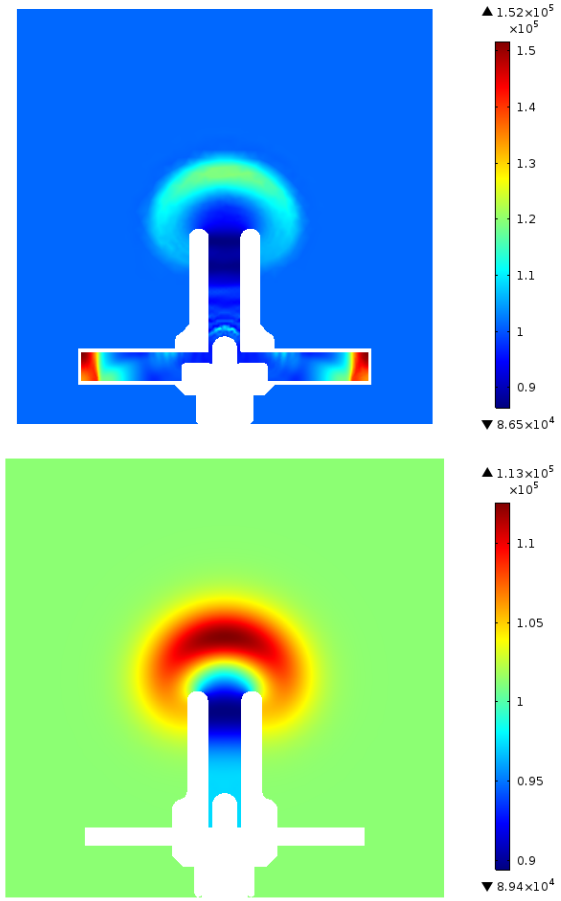

Figure 4. Pressure distribution at time of 100 µs for lightning current of 3 kA. Top - Chamber 1 (hollow electrodes), bottom (solid electrodes) - Chamber 2.

where h is the Planck constant, c the velocity of light, and k_B the Boltzmann constant. This equation is typically solved by the Discrete Ordinate Method (DOM). Since absorption coefficient is strongly frequency dependent, it is necessary to use a multi-band approach with averaged absorption coefficients. The most important effect is that high frequencies are strongly absorbed, whereas low frequencies are not so it was decided to use a simple two-band model. The first frequency band has a wavelength starting from zero up to $\lambda = 120\,\text{nm}$ and an absorption coefficient of $\alpha = 2000\,\text{m}^{-1}$, the second band starts from $\lambda = 120\,\text{nm}$ up to $\lambda = 1\,\text{mm}$ with $\alpha = 50\,\text{m}^{-1}$ [7].

3. Preliminary results.

3.1. Investigation of residual resistance.

As a preliminary step simulations with lightning pulse only applied to chamber (meaning no circuit interaction involved) were conducted for several chamber designs. For further simplification 3D-geometry was replaced by 2D assuming planar flow. Turbulence is neglected as well. Since arc quenching was not simulated directly the perfomance of different chamber geometries was evaluated on the basis of residual resistance assuming the lower the latter the more

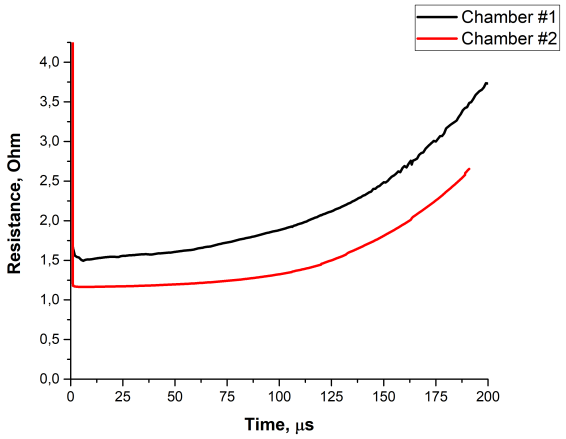

Figure 5. Resistanse curves for two different chambers. Black curve - upper chamber, red curve - lower chamber (see Fig. 4).

chances to prevent follow current to flow. The current pulse was imposed on chamber, its rise time and half-width were set to 8 µs and 50 µs correspondingly while magnitude was set to 3 kA. Results obtained for two previously tested chambers (Fig. 2) are depicted in Fig. 4 and Fig. 5 where the former displays pressure distribution at time about 100 µs while the latter displays resistance curve. The upper chamber in Fig. 4 corresponds to Chamber 1 on Fig. 5 and as it can be seen outperforms Chamber 2 (lower chamber) in terms of resistance rise rate. This result is in accordance with experimental knowledge.

3.2. Arc-circuit interaction

In order to simulate arc quenching (1)–(3) were coupled with circuit equations [7]. The circuit is depicted in Fig. 6, it represents simplified model of power grid. The capacitor C_0 is initially charged by voltage U_c which in fact stands for powerline nominal voltage so appearance of ZQ or IQ is dependent on the value of U_c. Indeed simulations gave different results for charging voltage values of 1 kV and 2 kV (Fig. 7 and Fig. 8 correspondingly). It can be seen from Fig. 7 that in case of 2 kV current vanishes only after approximately 5 ms while in case of 1 kV current hardly ever starts to flow and is interrupted after about 300 µs.

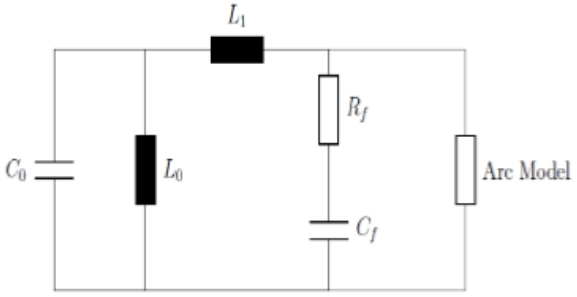

Figure 6. Electrical circuit model used for arc quenching simulations.

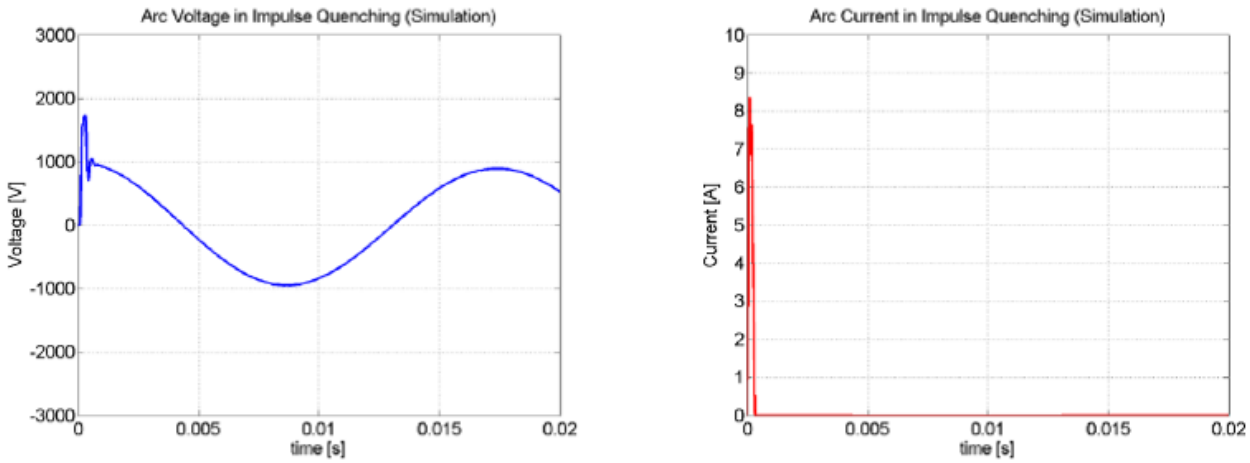

Figure 7. Current and voltage curves for $U_c = 1\,kV$.

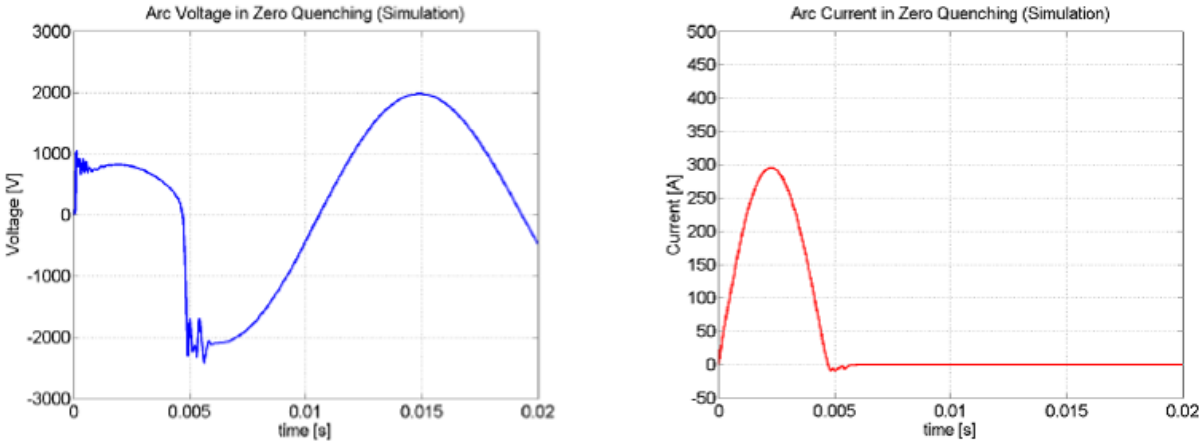

Figure 8. Current and voltage curves for $U_c = 2\,kV$.

4. Conclusions

Simulations of arc quenching in MCS were carried out with the help of specially developed impulse arc model based on MHD equations. Two important results should be highlighted. First, simulation results qualitatively match the experimental data. Second,full arc model with involved arc-circuit interaction demonstrated the transition from ZQ to IQ mode. Those promising achievements allow to consider simulation as a prospective tool for future MCS design optimization.

References

[1] G. Podporkin et al. Overhead lines lightning protection by multi-chamber arresters and insulator-arresters. *IEEE Transactions on Power Delivery*, 26(1):214–221, 2011. doi:10.1109/TPWRD.2010.2076368.

[2] G. Podporkin et al. Development of multi-chamber insulator-arresters for lightning protection of 220 kV overhead transmission lines. *XI SIPDA*, pages 160–165, 2011. doi:10.1109/SIPDA.2011.6088440.

[3] A. Gleizes et al. Thermal plasma modelling. *Journal of Physics D: Applied Physics*, 38(9):R153–R183, 2005. doi:10.1088/0022-3727/38/9/R01.

[4] F. Yang et al. Low-voltage circuit breaker arcs-simulation and measurements. *Journal of Physics D: Applied Physics*, 46(27):273001, 2013. doi:10.1088/0022-3727/46/27/273001.

[5] A. Cressault et al. Properties of air-aluminum thermal plasmas. *Journal of Physics D: Applied Physics*, 45(26):265202, 2012. doi:10.1088/0022-3727/45/26/265202.

[6] P. Kloc et al. Radiation transfer in air and air-Cu plasmas for two temperature profiles. *Journal of Physics D: Applied Physics*, 48(5):055208, 2015. doi:10.1088/0022-3727/48/5/055208.

[7] M. Mürmann et al. Modeling and simulation of the current quenching behavior of a line lightning protection device. *Journal of Physics D: Applied Physics*, 50(10):105203, 2017. doi:10.1088/1361-6463/aa560e.